



Title	Study on a metal-insulator-silicon hydrogen sensor with LaTiON as gate insulator
Author(s)	Yu, J; Chen, G; Lai, PT
Citation	
Issued Date	2013
URL	http://hdl.handle.net/10722/192462
Rights	Creative Commons: Attribution 3.0 Hong Kong License

Study on a Metal–Insulator–Silicon Hydrogen Sensor With LaTiON as Gate Insulator

Jerry Yu, Gang Chen, and Pui To Lai

Abstract—In this paper, by using a metal–insulator–semiconductor Schottky-diode structure, we examined the electrical and hydrogen-sensing properties of radio frequency sputtered LaTiON thin films that had been annealed at four different temperatures (450 °C, 550 °C, 650 °C, and 750 °C). Characterization of their morphological surface indicates that their average surface roughness decreases from 0.108 to 0.090 nm with increasing annealing temperature. X-ray diffraction shows the growths of La and Ti are in the 1 0 0 direction, i.e., in parallel to the Si substrate. Analysis of measured electrical characteristics indicates that thermionic emission is the dominant mechanism at low temperatures (from RT to 150 °C), while Poole–Frenkel emission plays an important role at high temperatures (above 150 °C) in the electrical conduction. Results suggest that the sample annealed at 650 °C has the most promising hydrogen-sensing performance (better current–voltage characteristics, higher sensitivity of 2.0 at 100 °C) among the four samples.

Index Terms—High- k dielectric, hydrogen, Schottky diode, sensor.

I. INTRODUCTION

THE awareness of climate change has prompted a scientific push towards a new and clean energy source to reduce the pollution to the environment. With this concern growing rapidly, scientists have examined hydrogen gas as a promising and realistic substance that can function as a fuel that one day can be implemented widely [1]–[3]. However, using such an explosive substance presents great risk and any leakage requires monitoring to prevent the occurrence of an ignition event [4].

As a consequence, it has become very important to study and develop hydrogen sensors with high sensitivity to detect this particular gas species with concentration down to parts per million and even parts per billion for the future energy industry. It is possible to develop one type of high-performance hydrogen sensors based on the structure of a metal-semiconductor Schottky diode [5]–[7]. Moreover, by

adding a thin insulating metal-oxide layer between its semi-conducting substrate and catalytic metal, the Schottky barrier height can be made dependent on the work function of the metal and the electron affinity of the metal oxide. Many reports in the literature have shown the advantages of using a thin metal oxide layer that is only several nanometers thick as it substantially improves the hydrogen-sensing performance of the Schottky-diode sensors [8]–[12].

For the fabrication of metal oxide-based thin films, RF sputtering has grown into one of the most mature and well-established physical deposition techniques. It is particularly advantageous for large-area film preparation and is relatively simple, straight forward and cost-effective. Since RF sputtering can deposit uniform thin films down to nanometer thicknesses, it is suitable for this research.

Lanthanum oxide has mostly been studied for dielectric applications [13], [14] and is also known to exhibit a particularly high dielectric constant of about 25 and large bandgap of 5.5 eV [15], which is advantageous in suppressing leakage current. Lanthanum itself, has primarily been used as a catalytic dopant in metal oxide materials such as (ZnO, SnO₂) in gas sensing [16]–[19]. Materials such as molybdenum oxide [20], tungsten oxide [21] and titanium oxide can have a much higher permittivity than La₂O₃ and TiO₂ has been examined particularly for its unique electrical and structural properties, exhibiting many advantages for gas sensing applications with a high dielectric constant of 80 and a bandgap of 3.3 eV [22]–[26]. These materials can be used to substitute silicon as the primary surface material and can exhibit far greater reactive changes in their electrical properties in the presence of hydrogen gas. Currently, the gas sensing properties of these two materials as a compound have yet to be examined and are still in its early stage of inquisition Hence in this work, we fabricated LaTi-based oxide thin film on Si substrate and examined its electrical properties and hydrogen sensing performance by using a metal-insulator-semiconductor Schottky-diode structure.

II. EXPERIMENTAL/METHODOLOGY

A. Fabrication

The sensors were fabricated on *n*-type silicon wafers (purchased from Silicon Quest International, USA) with an orientation of <100> and were diced into 10×10 mm² square substrates. The wafers were cleaned using the conventional RCA method: solution I (H₂O-H₂O₂-NH₄OH) and solution II (H₂O-H₂O₂-HCl) followed by dipping the wafers into 2% HF

Manuscript received August 2, 2012; revised November 13, 2012; accepted December 6, 2012. Date of publication January 4, 2013; date of current version March 26, 2013. This work was supported in part by the Research Grants Council (RGC) of Hong Kong Special Administrative Region (HKSAR), China, under Project HKU 713510E, and in part by the University of Hong Kong Development Fund (Nanotechnology Research Institute, 00600009). The associate editor coordinating the review of this paper and approving it for publication was Prof. Elliott R. Brown.

The authors are with the Department of Electrical and Electronic Engineering, University of Hong Kong, Hong Kong (e-mail: jcwylu@hku.hk; chengang@eee.hku.hk; laip@eee.hku.hk).

Color versions of one or more of the figures in this paper are available online at <http://ieeexplore.ieee.org>.

Digital Object Identifier 10.1109/JSEN.2012.2235065

for 1 min to remove the native oxide. The sputtering deposition was immediately performed after the cleaning procedure as explained below.

A La_2O_3 target (99.99% purity) and a Ti target (99.995% purity) (K.J Lesker) were placed into a Denton Vacuum Discovery sputterer. The chamber was pumped down to an operating pressure of 4.5×10^{-6} Torr. The sputtering of La_2O_3 and Ti was performed simultaneously by RF sputtering (at 30 W) of La_2O_3 and DC sputtering (at 0.12 A) of Ti for a duration of 16 s in a mixed Ar/ N_2 ambient (ratio = 24:8), which incorporated nitrogen in the oxide film to improve its thermal stability and reduce its leakage current. The substrates were also rotated at a rate of 3 rpm to enhance the film uniformity during deposition. The thickness of the as-deposited sputtered films was measured as 4.1 nm using a J.A. Woollam Co. VB400 ellipsometer.

Arrays of circular Pt pads (0.5-mm diameter) were deposited via DC sputtering (0.2 A for 10 min) using a shadow mask. The samples were annealed in a tube furnace (Lenton Thermal Design Ltd) at four different temperatures (450 °C, 550 °C, 650 °C and 750 °C) respectively for 10 min in a pure N_2 gas with a flow rate of 1000 mL/min.

The back oxide of the samples was removed by 20% HF and then they were blown dry with N_2 after rinsing in DI water. Subsequently, the samples were pasted onto headers via Ag epoxy and annealed in an oven at 200 °C for 30 min. Lastly, the front electrode of the sensor and one of the pins of the header were connected by a gold wire using a hybrid wedge bonder.

B. Characterization Methodology

The surface morphology and the crystallographic structure of the as-deposited samples were characterized by atomic force microscopy (AFM) and X-ray diffraction (XRD), respectively. Analysis of the samples will be presented in the Characterization section

C. Electrical and Gas Testing Procedure

Electrical and hydrogen-sensing measurements were performed using a computer-controlled measurement system consisting of a semiconductor parameter analyzer (HP 4145B), a thermostat-controlled chamber and two gas-flow controllers connected to a data acquisition PC unit. The mounted sample was placed into the stainless-steel chamber, and then H_2 and N_2 gases were injected accordingly.

III. CHARACTERIZATION

A. Surface Morphology

Fig. 1 shows a three-dimensional map of a $1 \mu\text{m} \times 1 \mu\text{m}$ section of the surface morphology of the LaTiON films. In this work, we designate the samples by their annealing temperature. The values of the parameters (surface roughness, mean grain size and mean grain diameter) measured by AFM are presented in Table I.

The results show a decreasing trend of the (1) average surface roughness, (2) mean grain size and (3) mean diameter

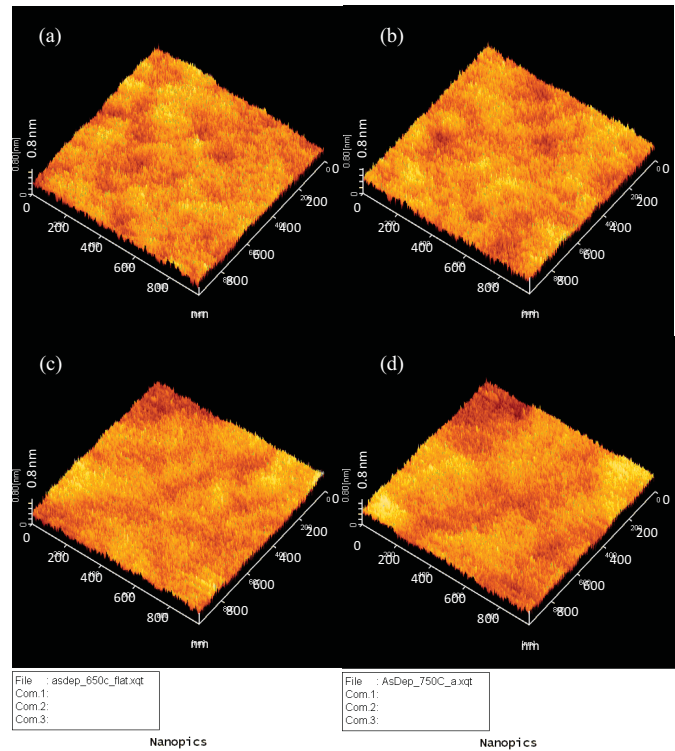


Fig. 1. 3-D AFM surface map of the LaTiON films annealed at (a) 450 °C, (b) 550 °C, (c) 650 °C, and (d) 750 °C.

TABLE I

PARAMETERS OF THE LaTiON FILMS (PREPARED UNDER DIFFERENT ANNEALING TEMPERATURES) MEASURED BY AFM

Annealing Temperature (°C)	450	550	650	750
Average Surface Roughness (nm)	0.108	0.107	0.095	0.090
Mean Grain Size (nm^2)	70.8	70.9	68.7	66.2
Mean Grain Diameter (nm)	9.5	9.5	9.3	9.2
Insulator Thickness (nm)	4.1	3.6	2.9	2.5

with respect to the increasing annealing temperature. With higher annealing temperature the LaTiON film is thinner due to stronger densification and therefore its surface becomes smoother.

B. Crystallographic Structure

Fig. 2 shows a plot of the XRD diffractogram presenting the measured data of the four LaTiON samples grown on Si substrate. The peaks of the plot appear to indicate the presence of elements which can be correlated to the peaks of the elements (ICDD card file) at their respective 2θ angles: [100] α -La at 56.52° [00-051-1165], [100] Ti at 55.65° [00-044-1288], and [110] TiN at 61.91° [03-065-0565]. The presence of LaTiO_3 [03-065-1385] and La_2O_3 [01-076-2273] peaks is overshadowed by the [100] Si peak at 69.13° [00-027-1402] due to the thin 4 nm layer. TiO_2 peaks can also be found at 69.36° and 69.49° [00-010-0063] inside this large Si peak. The results suggest that the growths of La and Ti follow in the direction of the [100] orientation of the substrate due to the nature of the film. Although there are many peaks that remain

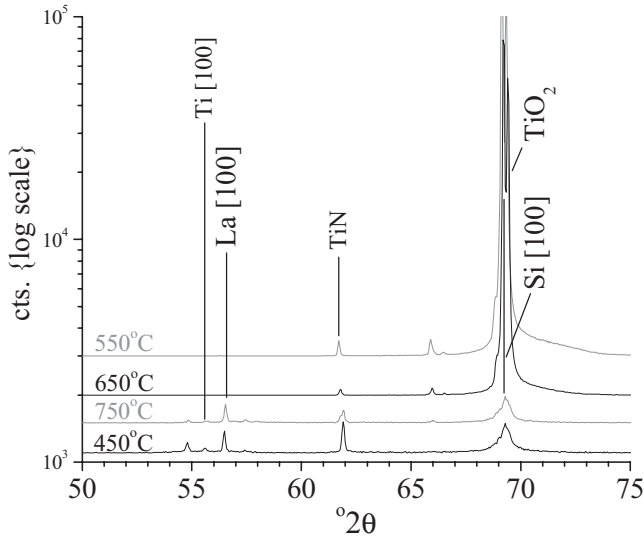


Fig. 2. XRD diffractogram of the LaTiON films annealed at different temperatures.

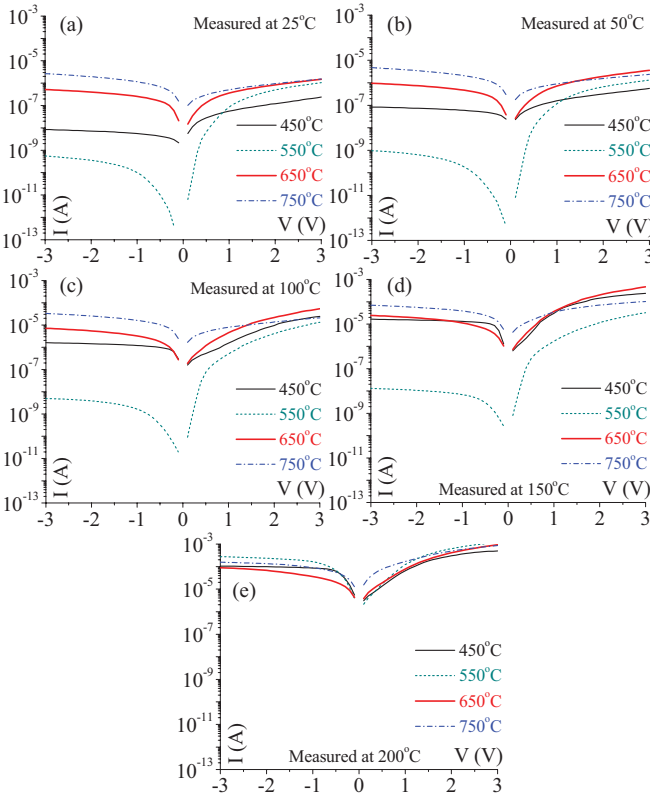


Fig. 3. I - V characteristics of the sensors (prepared under different annealing temperatures) measured at (a) 25 °C, (b) 50 °C, (c) 100 °C, (d) 150 °C, and (e) 200 °C.

ambiguous, it is possible that Si-O₂ or other compounds (TiSi, LaSi) could be present.

IV. ELECTRICAL PROPERTIES

A. Current-Voltage (I - V) Characteristics

The I - V characteristics of the Schottky-diode sensors measured at different temperatures from 25 °C to 200 °C are shown

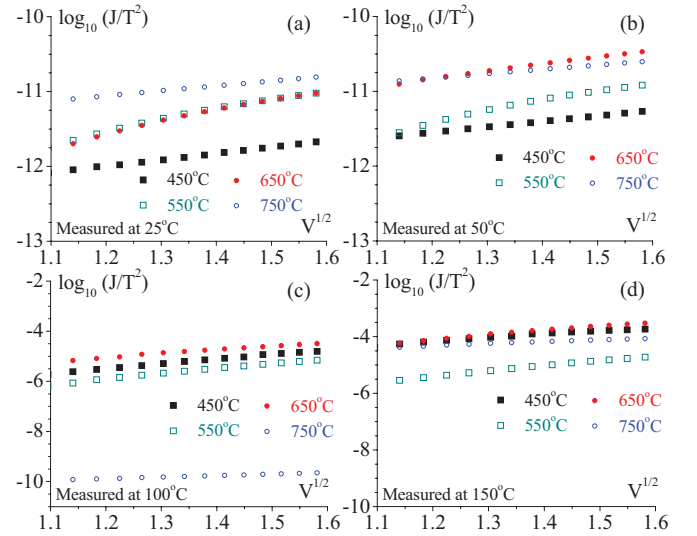


Fig. 4. Thermionic emission plot of the 4 sensors (prepared under different annealing temperatures) measured at (a) 25 °C, (b) 50 °C, (c) 100 °C, and (d) 150 °C.

in Fig. 3. The turn-on voltage for the 450 °C, 550 °C and 650 °C samples can be found to be 1.26, 0.97 and 0.95 V, respectively.

The carrier transport mechanism from the Si substrate through the thin metal oxide layer to the Pt metal can be described by the thermionic emission (TE) and Poole-Frenkel (PF) emission. Analysis of the results shows that the TE and PF emissions are most likely to contribute to the overall conduction mechanism.

B. Analysis of Thermionic Emission

The forward electrical characteristics can be described in terms of the Schottky J - V equation, when $V_F > 3kT/q$ [27]–[29]:

$$J_F = A^{**} T^2 \exp\left[\frac{-q\phi_B}{kT}\right] \exp\left[\frac{qV_F}{kT}\right] \quad (1)$$

where J_F is the forward current density; A^{**} is the effective Richardson constant; T is the absolute temperature; q is the electron charge; ϕ_B is the forward barrier height; and k is the Boltzmann's constant.

The forward barrier height can be calculated using the extrapolation method [27] and is given by the equation:

$$\phi_{B(FWD)} = \frac{kT}{q} \ln\left[\frac{A^{**} T^2}{J_0}\right]. \quad (2)$$

The thermionic emission plot based on the I - V data of the four sensors is shown in Fig. 4.

C. Analysis of Poole-Frenkel Emission

The PF emission, a trap-assisted mechanism, occurs when charge carriers travel through an insulator by trapping and de-trapping processes. It is a dominant conduction process in an insulator with a high trap density. The Poole-Frenkel current-voltage characteristics are given by [28], [29]:

$$I = B \exp\left[\frac{\beta V^{1/2} - \Phi_t}{k_B T}\right] \quad (3)$$

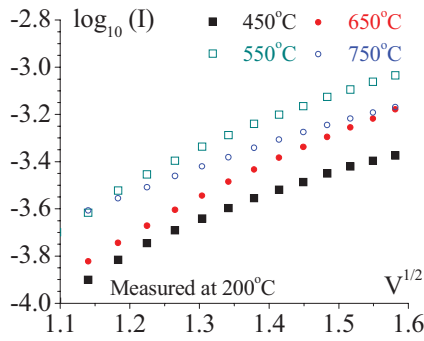


Fig. 5. Poole–Frenkel emission plot of the four sensors (with different annealing temperatures) measured at 200 °C.

TABLE II

CONSTANTS OF LaTiON FILM EXTRACTED FROM THE POOLE–FRENKEL PLOT OF THE SENSORS (PREPARED UNDER DIFFERENT ANNEALING TEMPERATURES) AT DIFFERENT OPERATING TEMPERATURES

Annealing Temperature (°C)	450	550	650	750
κ (at 25 °C)	32.8	21.9	24.0	36.6
κ (at 50 °C)	34.1	21.5	27.5	37.4
κ (at 100 °C)	21.2	16.1	20.6	33.9
κ (at 150 °C)	24.8	18.9	19.4	31.8
κ (at 200 °C)	23.0	18.4	18.5	24.1

where $\beta = (q^3/(\pi\kappa \epsilon_0 t_{ox}))^{1/2}$; Φ_1 is the depth of the trap potential well; B is a physical parameter; κ is the dielectric constant of the insulator; k_B is the Boltzmann’s constant; ϵ_0 is the permittivity of free space; and t_{ox} is the oxide thickness.

The base-10 logarithm of equation (3) has the form:

$$\log I = \frac{\log(B) - \Phi_1}{2.3k_B T} + \frac{\beta V^{1/2}}{2.3k_B T}. \quad (4)$$

The Poole-Frenkel plot based on the I - V data is presented in Fig. 5, and the corresponding value of the dielectric constant κ extracted from the measured data using equation (4) is given in Table II.

As can be seen, the extracted κ values for the LaTiON films are in the range from 16.1 to 37.4. The values for pure La₂O₃ films in the literature are 18.8 [30], 26.0 [31], and 25.0 [28]. Since all the samples in this work show a κ value within the reported range by other authors only at the operating temperature of 200 °C, this signifies that the Poole-Frenkel emission should contribute as the dominant conduction process in these samples in the high-temperature range (> 150 °C). This phenomenon was also observed in other works [29]–[31] because at high temperature, electrons confined in the oxide traps can have sufficient thermal energy to escape, contributing to extra current flow. Since TiO₂ has much higher κ value (~75 as reported in [32]) than La₂O₃ adding Ti to La₂O₃ in this work should result in a higher κ value, e.g. 33 in [33]. However, due to inevitable growth of a low- κ layer at the LaTiON/substrate interface during the annealing step, the effective κ value of the two layers combined is lower, e.g. ~18 to 25 in [34]. Therefore, the κ value of ~20 for our samples extracted from the Poole Frenkel model is a reasonable value.

TABLE III

PARAMETERS OF LaTiON FILMS (PREPARED UNDER DIFFERENT ANNEALING TEMPERATURES) AS EXTRACTED FROM THE TE AND PF PLOTS

Annealing Temperature (°C)	450	550	650	750
Barrier height (eV)	0.74	0.73	0.72	0.71
Trap Energy (eV)	0.59	0.58	0.58	0.57

In this study, the conduction mechanism of the LaTiON films is also analyzed by fitting the I - V data to the thermionic emission and Poole-Frenkel emission models with the method used by Lee *et al.* [33]. By extrapolating the data with respect to $1/T$, the barrier height and trap center level are calculated and their values are as given in Table III. During the calculation of the barrier height, we neglected the 200 °C data set in order to achieve a value which is consistent across the four samples because the difference in annealing temperature mainly affects the number of traps in the metal oxide. If we include the results at 200 °C, the values for the calculated barrier heights of the 4 samples would differ significantly, and therefore the results become unreasonable. This indicates that TE should be the dominant mechanism between 25 °C and 150 °C. Combining with the analysis on the extracted κ values in the previous paragraph, it can be inferred that at around 200 °C, the traps in the oxide are thermally activated and cause a gradual change in the dominant conduction mechanism from the TE emission to the PF emission.

A flatband voltage of 1.06 V (the work-function difference between Pt and the Si substrate) is used in the calculations. The results clearly show that the barrier height and the energy level of the trap center are independent of the annealing temperature because the annealing temperature should mainly affect the number of traps in the oxide film. It also indicates that both Poole-Frenkel and Schottky emission models can be involved in the actual conduction mechanism.

V. HYDROGEN SENSING PERFORMANCE

A. Barrier Height Variation

The LaTiON-based sensors were exposed to hydrogen gas (with a concentration of 1001 ppm) and their I - V characteristics were measured at different temperatures (from 25 to 200 °C) as shown in Fig. 6.

Fig. 6 shows the I - V characteristics of the samples (at different operating temperatures up to 200 °C) before and after exposure to hydrogen (at 1001 ppm concentration). Fig. 6a, 6c and 6d also show that at 200 °C, the characteristics under H₂ exposure become less conductive than those under air exposure, which indicates that the Schottky barrier breaks down and most likely the Si sensors are damaged at 200 °C. Due to the very small thickness of the metal-oxide layer, the barrier is insufficient to inhibit the highly energetic electrons to flow uncontrollably over the barrier. The I - V characteristics of the sensor in Fig. 6b illustrate an explicit breakdown of the Schottky barrier as its conductivity begins to decline at 200 °C.

In general, the operation of the sensors is based on the Schottky barrier-height lowering mechanism upon exposure

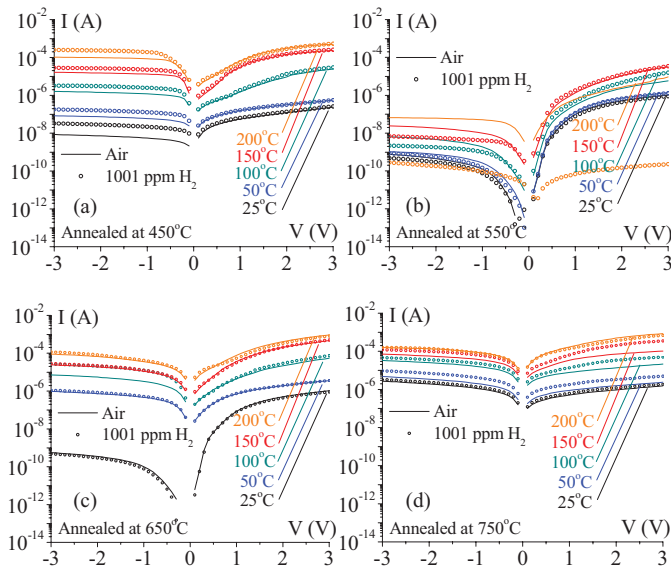


Fig. 6. I–V characteristics of the sensors at different operating temperatures and as exposed to air and H₂ with 1001 ppm concentration, prepared under different annealing temperatures of (a) 450 °C, (b) 550 °C, (c) 650 °C, and (d) 750 °C.

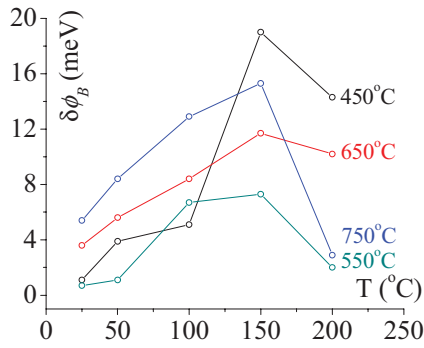


Fig. 7. Plot of the barrier height variation with respect to operating temperature for the sensors prepared under different annealing temperatures of (a) 450 °C, (b) 550 °C, (c) 650 °C, and (d) 750 °C.

to hydrogen gas [34]. Hydrogen molecules are adsorbed and then dissociated into H atoms at the surface of the catalytic Pt metal. These H atoms then diffuse through the Pt and accumulate at the Pt/metal-oxide interface. As a result, a dipole charge is formed at the interface and causes a lowering of the barrier height. The change in barrier height (barrier-height variation) upon exposure to H₂ gas is calculated using the extrapolation method [27]. The results in Fig. 7 indicate that the largest change occurs at an operating temperature of 150 °C, and the sample annealed at 450 °C exhibits the largest change among the four samples.

B. Sensitivity

A plot of the sensitivity (with respect to 1001-ppm H₂ in N₂) for the samples (annealed at 450 °C, 550 °C, 650 °C and 750 °C) at different operating temperatures is shown in Fig. 8. For a Schottky diode, its sensitivity S is defined in equation (4) as [35], [36]:

$$S = \frac{I_{H_2} - I_{Air}}{I_{Air}} \quad (5)$$

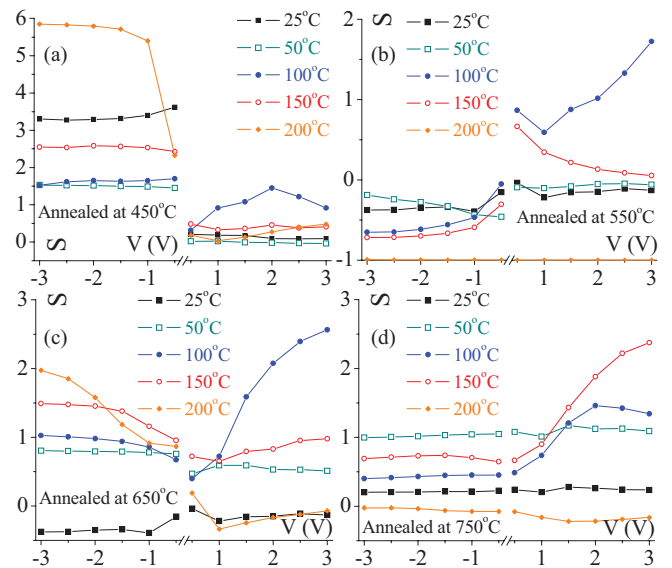


Fig. 8. Plot of the sensitivity with respect to bias voltage at different operating temperatures for the sensors prepared under annealing temperatures of (a) 450 °C, (b) 550 °C, (c) 650 °C, and (d) 750 °C.

where I_{H_2} and I_{Air} are the currents of the device in hydrogen and air respectively.

The sensitivity of the samples annealed at 550 °C, 650 °C, and 750 °C exhibits increasing trend with respect to increasing forward bias voltage at elevated operating temperatures. In Fig. 8a the sample annealed at 450 °C indicates a steady sensitivity over a range of voltage (at different operating temperatures), within a range of 6.0 under reverse bias and up to 1.5 under forward bias. This is also similar in the reverse region of the sample annealed at 750 °C. Fig. 8b and Fig. 8c show that the sensitivity can have a negative value. This signifies the current caused by thermal generation of carriers overshadows the current induced by the lowered barrier (as caused by the hydrogen dipole layer at the metal/insulator interface). Both conduction mechanisms (Thermionic Emission and Poole-Frenkel) are equally significant at around 150 °C, which implies that the lowering of barrier height allows carriers with lower energies to flow over the barrier and also through the thin dielectric via the traps. The plots in Fig. 8, suggest that the annealing at temperature between 450 °C and 650 °C causes the formation of interface traps, which provide low-energy carriers (at 100 °C and 150 °C) with a route to flow easily through the thin dielectric via the Poole-Frenkel mechanism. As the barrier is lowered by the hydrogen dipole layer, these low-energy carriers are more likely to flow over the barrier via thermionic emission, with some of them still flowing through the thin dielectric via the trap-assisted mechanism simultaneously.

VI. HYDROGEN SENSING PERFORMANCE

A. Dynamic Response

The dynamic response of the sensors under a reverse bias is presented in Fig. 9 at an operating temperature of 100 °C. The results show that by depositing a thin layer of LaTiON on Si, the sensor is more responsive towards hydrogen, and it is

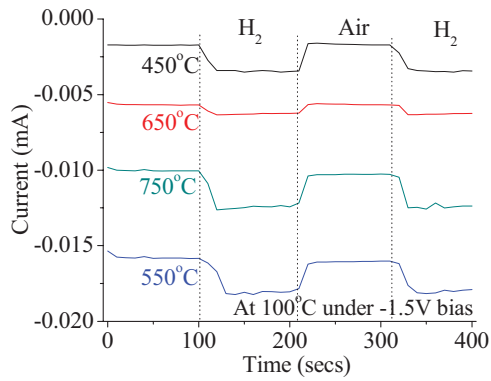


Fig. 9. Dynamic response of the sensors (prepared under different annealing temperatures) operating at 100 °C under -1.5 V voltage bias.

possible to increase the dynamic response in future study by using different substrate materials such as SiC or GaN, which can withstand higher operating temperature. We have shown that thin LaTiON films deposited on Si and annealed at four different temperatures can exhibit different hydrogen sensing properties.

VII. CONCLUSION

In this work, nanometer-thick LaTiON thin films sputtered on Si substrate were examined for their electrical and hydrogen-sensing properties by using a metal-insulator-semiconductor Schottky-diode structure. AFM results indicate a decrease in surface roughness (from 0.108 nm to 0.090 nm) with increasing annealing temperature (from 450 °C to 750 °C), while XRD shows the growths of La and Ti in the direction of the Si substrate. We discuss the effects of annealing on the films and how it affects the sensing performance of the sensors. Analysis on the measured I - V characteristics of the samples indicates that thermionic emission controls their electrical conduction from RT to 150 °C while Poole-Frenkel emission is the dominant mechanism beyond 150 °C. These results show that by incorporating La and Ti together as the insulator layer, the resulting sensors can exhibit good sensing behavior towards hydrogen gas. The hydrogen-sensing properties of the samples indicate a promising sensitivity (~ 2.0 at 100 °C for the sample annealed at 650 °C), and their dynamic response, sensitivity, and maximum operating temperature could be further improved in future work by using a different substrate (e.g. SiC or GaN).

REFERENCES

- [1] V. G. Dovi, F. Friedler, D. Huisingh, and J. J. Klemes, "Cleaner energy for sustainable future," *J. Cleaner Prod.*, vol. 17, no. 10, pp. 889–895, Jul. 2009.
- [2] B. C. R. Ewan and R. W. K. Allen, "A figure of merit assessment of the routes to hydrogen," *Int. J. Hydrogen Energy*, vol. 30, no. 8, pp. 809–819, Jul. 2005.
- [3] P. Moriarty and D. Honnery, "Hydrogen's role in an uncertain energy future," *Int. J. Hydrogen Energy*, vol. 34, no. 1, pp. 31–39, Jan. 2009.
- [4] X. Bevenot, A. Trouillet, C. Veillas, H. Gagnaire, and M. Clément, "Hydrogen leak detection using an optical fibre sensor for aerospace applications," *Sens. Actuators B, Chem.*, vol. 67, nos. 1–2, pp. 57–67, Aug. 2000.
- [5] S. Shukla, S. Seal, L. Ludwig, and C. Parish, "Nanocrystalline indium oxide-doped tin oxide thin film as low temperature hydrogen sensor," *Sens. Actuators B, Chem.*, vol. 97, nos. 2–3, pp. 256–265, Feb. 2004.
- [6] B. P. Luther, S. D. Wolter, and S. E. Mohny, "High temperature Pt Schottky diode gas sensors on n-type GaN," *Sens. Actuators B, Chem.*, vol. 56, nos. 1–2, pp. 164–168, Jun. 1999.
- [7] J. Schallwig, G. Muller, U. Karrer, M. Eickhoff, O. Ambacher, M. Stutzmann, L. Görgens, and G. Dollinger, "Hydrogen response mechanism of Pt-GaN Schottky diodes," *Appl. Phys. Lett.*, vol. 80, no. 7, pp. 1222–1224, Feb. 2002.
- [8] C. C. Cheng, Y. Y. Tsai, K. W. Lin, H.-I. Chen, W.-H. Hsu, H.-M. Chuang, C.-Y. Chen, and W.-C. Liu, "Hydrogen sensing characteristics of Pd- and Pt- $\text{Al}_{0.3}\text{Ga}_{0.7}\text{As}$ metal-semiconductor (MS) Schottky diodes," *Semicond. Sci. Technol.*, vol. 19, no. 6, pp. 778–782, Jun. 2004.
- [9] C. C. Cheng, Y. Y. Tsai, K. W. Lin, H.-I. Chen, C.-T. Lu, and W.-C. Liu, "Hydrogen sensing characteristics of a Pt-oxide- $\text{Al}_{0.3}\text{Ga}_{0.7}\text{As}$ MOS Schottky diode," *Sens. Actuators B, Chem.*, vol. 99, nos. 2–3, pp. 425–430, May 2004.
- [10] C. W. Hung, H. L. Lin, H. I. Chen, Y.-Y. Tsai, P.-H. Lai, S.-I. Fu, and W.-C. Liu, "A novel Pt/ $\text{In}_{0.52}\text{Al}_{0.48}\text{As}$ Schottky diode-type hydrogen sensor," *IEEE Electron Device Lett.*, vol. 27, no. 12, pp. 951–954, Dec. 2006.
- [11] K. W. Lin, H. I. Chen, C. T. Lu, Y.-Y. Tsai, H.-M. Chuang, C.-Y. Chen, and W.-C. Liu, "A hydrogen sensing Pd/ InGaP metal-semiconductor (MS) Schottky diode hydrogen sensor," *Semicond. Sci. Technol.*, vol. 18, no. 7, pp. 615–619, Jul. 2003.
- [12] Y. Y. Tsai, K. W. Lin, C. T. Lu, H.-I. Chen, H.-M. Chuang, C.-Y. Chen, C.-C. Cheng, and W.-C. Liu, "Investigation of hydrogen-sensing properties of Pd/ AlGaAs -based Schottky diodes," *IEEE Trans. Electron Devices*, vol. 50, no. 12, pp. 2532–2539, Dec. 2003.
- [13] S. Guha, E. Cartier, M. A. Gribelyuk, N. A. Bojarczuk, and M. C. Copel, "Atomic beam deposition of lanthanum- and yttrium-based oxide thin films for gate dielectrics," *Appl. Phys. Lett.*, vol. 77, no. 17, pp. 2710–2712, Oct. 2000.
- [14] J. P. Maria, D. Wicaksana, A. I. Kingon, B. Busch, H. Schulte, E. Garfunkel, and T. Gustafsson, "High temperature stability in lanthanum and zirconia-based gate dielectrics," *J. Appl. Phys.*, vol. 90, no. 7, pp. 3476–3482, Oct. 2001.
- [15] J. Robertson, "Maximizing performance for higher K gate dielectrics," *J. Appl. Phys.*, vol. 104, no. 12, pp. 124111-1–124111-7, Dec. 2008.
- [16] A. Marsal, A. Cornet, and J. R. Morante, "Study of the CO and humidity interference in La doped tin oxide CO_2 gas sensor," *Sens. Actuators B, Chem.*, vol. 94, no. 3, pp. 324–329, Oct. 2003.
- [17] I. Stambolova, K. Konstantinov, S. Vassilev, P. Peshev, and T. Tsacheva, "Lanthanum doped SnO_2 and ZnO thin films sensitive to ethanol and humidity," *Mater. Chem. Phys.*, vol. 63, no. 2, pp. 104–108, Feb. 2000.
- [18] E. Traversa, S. Matsushima, G. Okada, Y. Sadaoka, Y. Sakai, and K. Watanabe, " NO_2 sensitive LaFeO_3 thin-films prepared by RF-sputtering," *Sens. Actuators B, Chem.*, vol. 25, nos. 1–3, pp. 661–664, Apr. 1995.
- [19] M. F. Vignolo, S. Duhalde, M. Bormioli, G. Quintana, M. Cervera, and J. Tocho, "Structural and electrical properties of lanthanum oxide thin films deposited by laser ablation," *Appl. Surf. Sci.*, vol. 197, pp. 522–526, Sep. 2002.
- [20] D. D. Yao, J. Z. Ou, K. Latham, S. Zhuiykov, A. P. O'Mullane, and K. Kalantar-Zadeh, "Electrodeposited α - and β -phase MoO_3 films and investigation of their gasochromic properties," *Cryst. Growth Design*, vol. 12, no. 4, pp. 1865–1870, Apr. 2012.
- [21] M. Breedon, P. Spizzirri, M. Taylor, J. du Plessis, D. McCulloch, J. Zhu, L. Yu, Z. Hu, C. Rix, W. Wlodarski, and K. Kalantar-Zadeh, "Synthesis of nanostructured tungsten oxide thin films: A simple, controllable, inexpensive, aqueous sol-gel method," *Cryst. Growth Design*, vol. 10, no. 1, pp. 430–439, Jan. 2009.
- [22] N. O. Savage, S. A. Akbar, and P. K. Dutta, "Titanium dioxide based high temperature carbon monoxide selective sensor," *Sens. Actuators B, Chem.*, vol. 72, no. 3, pp. 239–248, Feb. 2001.
- [23] C. Lu, and Z. Chen, "High-temperature resistive hydrogen sensor based on thin nanoporous rutile TiO_2 film on anodic aluminum oxide," *Sens. Actuators B, Chem.*, vol. 140, no. 1, pp. 109–115, Jun. 2009.
- [24] T. Usagawa and Y. Kikuchi, "A Pt-Ti-O gate Si-metal-insulator-semiconductor field-effect transistor hydrogen gas sensor," *J. Appl. Phys.*, vol. 108, no. 7, pp. 074909-1–074909-8, Oct. 2010.
- [25] J. Robertson, "High dielectric constant oxides," *Eur. Phys. J., Appl. Phys.*, vol. 28, no. 3, pp. 265–291, Dec. 2004.
- [26] J. Robertson, "High dielectric constant gate oxides for metal oxide Si transistors," *Rep. Progr. Phys.*, vol. 69, no. 2, pp. 327–396, Feb. 2006.

- [27] S. Sze and K. K. Ng, *Physics of Semiconductor Devices*, 3rd ed. New York: Wiley, 2008.
- [28] C. Y. Chang and S. M. Sze, "Carrier transport across metal-semiconductor barriers," *Solid-State Electron.*, vol. 13, no. 6, pp. 727–740, 1970.
- [29] W. Monch, "Metal-semiconductor contacts: Electronic-properties," *Surf. Sci.*, vol. 299, nos. 1–3, pp. 928–944, Jan. 1994.
- [30] J. H. Jun, D. J. Choi, K. H. Kim, K. Y. Oh, and C. J. Hwang, "Effect of structural properties on electrical properties of lanthanum oxide thin film as a gate dielectric," *Jpn. J. Appl. Phys.*, vol. 42, no. 6A, pp. 3519–3522, Jun. 2003.
- [31] V. Capodiceci, F. Wiest, T. Sulima, J. Schulze, and I. Eisele, "Examination and evaluation of La_2O_3 as gate dielectric for sub-100 nm CMOS and DRAM technology," *Microelectron. Rel.*, vol. 45, nos. 5–6, pp. 937–940, 2005.
- [32] M. Kadoshima, M. Hiratani, Y. Shimamoto, K. Torii, H. Miki, S. Kimura, and T. Nabatame, "Rutile-type TiO_2 thin film for high-k gate insulator," *Thin Solid Films*, vol. 424, no. 2, pp. 224–228, Jan. 2003.
- [33] H.-J. Lee, C. Ahn, and S. Kang, "DC conduction behavior of $\text{Bi}_{3.15}\text{Nd}_{0.85}\text{Ti}_3\text{O}_{12}$ thin films grown by RF-magnetron sputtering," *J. Electroceram.*, vol. 21, no. 1, pp. 851–854, 2008.
- [34] L. G. Ekedahl, M. Eriksson, and I. Lundstrom, "Hydrogen sensing mechanisms of metal-insulator interfaces," *Accounts Chem. Res.*, vol. 31, no. 5, pp. 249–256, May 1998.
- [35] S. Kim, B. S. Kang, F. Ren, K. Ip, Y. W. Heo, D. P. Norton, and S. J. Pearton, "Sensitivity of Pt/ZnO Schottky diode characteristics to hydrogen," *Appl. Phys. Lett.*, vol. 84, no. 10, pp. 1698–1700, Mar. 2004.
- [36] X. F. Chen, W. G. Zhu, and O. K. Tan, "Microstructure, dielectric properties and hydrogen gas sensitivity of sputtered amorphous $\text{Ba}_{0.67}\text{Sr}_{0.33}\text{TiO}_3$ thin films," *Mater. Sci. Eng. B, Solid State Mater. Adv. Technol.*, vol. 77, no. 2, pp. 177–184, Aug. 2000.

Jerry Yu received a double degree in applied physics and electronic engineering and the Ph.D. degree from RMIT University, Melbourne, Australia, in 2007 and 2011, respectively.

He is a Post-Doctoral Fellow with The University of Hong Kong, Hong Kong. He investigates the physical, electronic and catalytic properties of these structures, and his work includes the development of new theoretical mechanisms to incorporate the effects exhibited by matter on the nanoscale. His current research interests include the design and fabrication of multiple quantum wells from thin film metal-oxide and metal-nitride films for the development of nanotechnology enabled hydrogen and hydrocarbon gas sensors.

Gang Chen received the Bachelors degree in engineering and the Masters degree in engineering from the Department of Electronic Science and Technology, Huazhong University of Science and Technology, Wuhan, China, in 2004 and 2006, respectively. He is currently pursuing the Ph.D. degree at the Department of Electrical and Electronic Engineering, The University of Hong Kong, Hong Kong.

His current research interests include on nanoelectronic devices, especially targeting the area of gas sensors.

Pui To Lai received the B.Sc. (Eng.) degree from the University of Hong Kong, Hong Kong. His Ph.D. research at the University of Hong Kong was on the design of small-sized MOS transistor with emphasis on narrow-channel effects. The work involved the development of both analytical and numerical models, the study of this effect in relation to different isolation structures, and the development of efficient numerical algorithms for device simulation.

He was a Post-Doctoral Fellow with the University of Toronto, where he proposed and implemented a novel self-aligned structure for bipolar transistor and designed and implemented an advanced poly-emitter bipolar process with emphasis on self-alignment and trench isolation. Current interests are on thin gate dielectrics for FET devices based on Si, SiC, GaN, Ge and organics; micro-sensors for detecting gases, heat, light and flow.